JACS Au
AN OPEN ACCESS JOURNAL OF THE AMERICAN CHEMICAL SOCIETY

pubs.acs.org/jacsau Perspective

Utilizing CO_2 as a Reactant for C_3 Oxygenate Production via Tandem Reactions

Akash N. Biswas, Lea R. Winter, Zhenhua Xie, and Jingguang G. Chen*

Cite This: *JACS Au* 2023, 3, 293−305 Read Online

ACCESS | Metrics & More | Article Recommendations | Supporting Information

ABSTRACT: One possible solution to closing the loop on carbon emissions is using CO_2 as the carbon source to generate high-value, multicarbon products. In this Perspective, we describe four tandem reaction strategies for converting CO_2 into C_3 oxygenated hydrocarbon products (i.e., propanal and 1-propanol), using either ethane or water as the hydrogen source: (1) thermocatalytic CO_2-assisted dehydrogenation and reforming of ethane to ethylene, CO, and H_2, followed by heterogeneous hydroformylation, (2) one-pot conversion of CO_2 and ethane using plasma-activated reactions in combination with thermocatalysis, (3) electrochemical CO_2 reduction to ethylene, CO, and H_2, followed by thermocatalytic hydroformylation, and (4) electrochemical CO_2 reduction to CO, followed by electrochemical CO reduction to C_3 oxygenates. We discuss the proof-of-concept results and key challenges for each tandem scheme, and we conduct a comparative analysis of the energy costs and prospects for net CO_2 reduction. The use of tandem reaction systems can provide an alternative approach to traditional catalytic processes, and these concepts can be further extended to other chemical reactions and products, thereby opening new opportunities for innovative CO_2 utilization technologies.

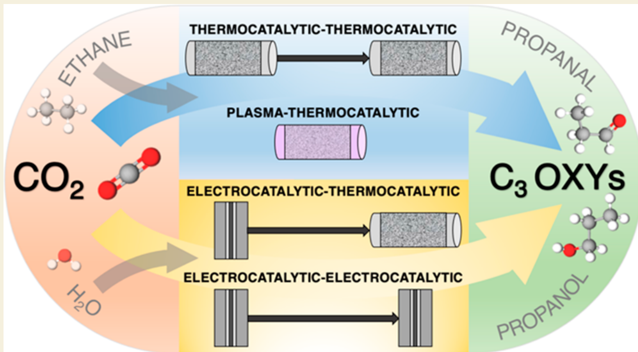

KEYWORDS: *CO_2 utilization, C_3 oxygenates, tandem reactors, thermocatalysis, electrocatalysis, plasma chemistry*

1. INTRODUCTION

To prevent the catastrophic, irreversible consequences of climate change, global warming should be limited to below 1.5 °C above preindustrial levels.[1] In addition to deep emission reductions, negative emission technologies that actively remove CO_2 from the atmosphere will also play a critical role. This can be accelerated with economical CO_2 conversion technologies that utilize CO_2 as the carbon source to produce value-added fuels and chemicals, which may result in net-negative CO_2 emissions when considering the avoided emissions associated with replacing fossil-fuel-derived products.

In particular, C_3 oxygenated hydrocarbons (C_3 Oxys), such as propanol and propanal, represent desirable products, since they are used as versatile solvents and feedstocks in many chemical industrial processes.[2,3] Propanol is also an excellent fuel additive because it has a higher octane number and heating value than methanol or ethanol, as well as lower emissions when it is combusted.[4] However, due to its complex production process, propanol currently has a higher market price and smaller global production volume (0.2 Mt/year) than other mass-produced chemicals such as methanol (150 Mt/year), ethanol (77 Mt/year), and ethylene (140Mt/year).[5] Therefore, the conversion of CO_2 to C_3 Oxys likely represents one of the shorter-term pathways to economic feasibility by displacing the existing conventional processes and making more immediate progress toward decarbonizing the chemicals industry. Furthermore, the global market usage of C_3 Oxy platform molecules for chemicals and fuels may increase if a cheaper, more sustainable production method emerges.

At present, C_3 Oxys are conventionally produced via hydroformylation (also known as oxo synthesis). However, the industrial high-pressure homogeneous hydroformylation process involves large energy costs due to the high pressures (10−30 atm) needed to obtain a high product yield, in addition to the energy required for product separation and homogeneous catalyst recovery.[6] Moreover, the feedstocks of ethylene and syngas (CO and H_2) are also generated using energy-intensive and carbon-emitting processes: ethylene is typically produced from thermal steam cracking of naphtha, crude oil, or natural gas, and syngas is primarily derived from natural gas steam reforming or coal gasification. The involvement of multiple independent process steps also leads

Received: September 26, 2022
Revised: December 1, 2022
Accepted: December 7, 2022
Published: January 13, 2023

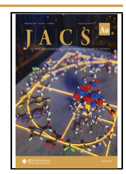

https://doi.org/10.1021/jacsau.2c00533
JACS Au 2023, 3, 293−305

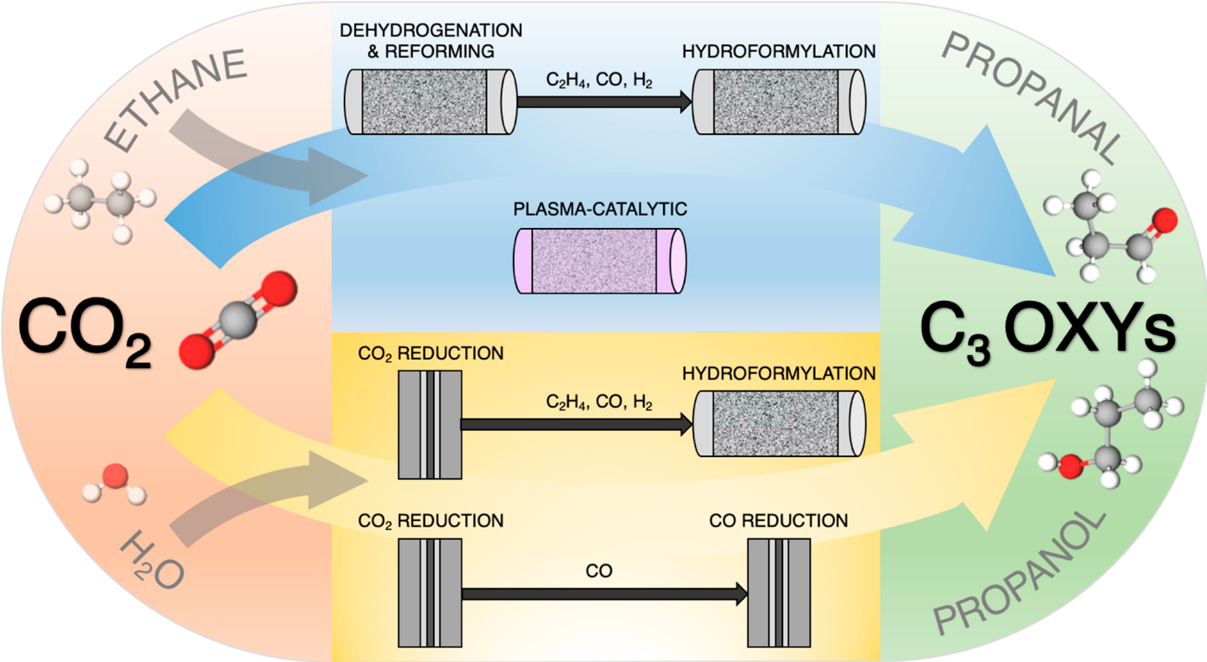

Figure 1. Schematic of tandem reaction strategies for converting CO_2 into C_3 oxygenated hydrocarbons. In the reaction schemes, C_3 oxygenated hydrocarbons (C_3 Oxys) are produced by reacting CO_2 with ethane via tandem thermocatalytic or one-pot plasma-catalytic conversion (top schemes, blue) or with H_2O via electrocatalytic reduction followed by thermocatalytic hydroformylation or electrocatalytic CO reduction (bottom schemes, yellow).

to operational challenges and safety risks during the transportation and storage of intermediate products (i.e., toxic syngas and flammable ethylene).

Instead, C_3 Oxy synthesis methods that can operate under mild conditions, utilize renewable carbon-free energy sources, and consume CO_2 as a reactant may provide more sustainable alternatives to traditional processes. The direct coupling of multiple reactors in a tandem configuration can also eliminate the separation, transportation, or storage steps that may otherwise be associated with obtaining hydroformylation feedstocks from separate, independent processes. In addition to CO_2 as the carbon source, a hydrogen source is necessary for oxygenate production. However, it is unlikely that the utilization of molecular H_2 can achieve a net reduction of CO_2. At present, ~95% of H_2 is derived from hydrocarbon-based feedstocks and generates CO_2 as a byproduct.[7] Furthermore, a previous CO_2 mass balance analysis for methanol synthesis using hybrid electrocatalytic and thermocatalytic schemes revealed that CO_2 conversion to methanol that requires H_2 as a reactant is net CO_2-positive even when using relatively decarbonized energy sources,[8] suggesting that CO_2 + H_2 to propanol should be even less effective for net CO_2 reduction due to selectivity issues. Alternatively, light alkanes (via thermal or plasma activation) or H_2O (via electrochemical activation) may be used as the hydrogen source for CO_2 conversion. However, CO_2 as well as alkanes/H_2O are thermodynamically stable and difficult (or nearly impossible) to convert directly into C_3 Oxys in a single reactor. Therefore, the application of tandem reaction strategies coupling thermocatalysis, electrocatalysis, or plasma catalysis is necessary for effectively upgrading CO_2 to C_3 Oxys.

In this Perspective, we consider four ambient-pressure tandem reaction pathways (Figure 1) for producing C_3 Oxys from CO_2, using either ethane or water as the hydrogen source: (1) thermocatalytic CO_2-assisted dehydrogenation and reforming of ethane to ethylene, CO, and H_2, followed by thermocatalytic heterogeneous hydroformylation (TC-TC),[9,10] (2) one-pot conversion of CO_2 and ethane using plasma-activated reactions in combination with thermocatalysis (P-TC),[11] (3) electrocatalytic CO_2 reduction to ethylene, CO, and H_2, followed by thermocatalytic hydroformylation (EC-TC),[12] and (4) electrocatalytic CO_2 reduction to CO, followed by electrocatalytic CO reduction (EC-EC).[13] We first introduce the relevant reactions and proof-of-concept results for the four different tandem schemes. Then, we compare the energy costs and prospects for net CO_2 reduction for each process. Finally, we discuss the key challenges and opportunities for tandem reaction systems.

2. TANDEM REACTION STRATEGIES FOR THE PRODUCTION OF C_3 OXYGENATED HYDROCARBONS

2.1. Upgrading CO_2 with Ethane

The supply of natural gas has increased significantly in recent decades as a result of advances in drilling and fracking techniques, as well as the discovery of large shale gas reserves (currently ~7.6 quadrillion cubic feet of global recoverable reserves).[7] The abundant supply, and therefore low prices, of natural gas has motivated efforts to upgrade light alkanes into value-added products. In particular, after methane, ethane represents the second most abundant component in shale gas deposits (3−16%), but it is typically underutilized.[14] Therefore, the abundant ethane in natural gas can be used as a carbon source as well as the hydrogen source to react with CO_2, instead of using CO_2-intensive H_2 derived from natural gas as the hydrogen source. The consumption of CO_2 as a coreactant with ethane obtained as surplus during natural gas extraction can potentially lead to a neutral or negative-emitting process (on the basis of carbon that has already been released

https://doi.org/10.1021/jacsau.2c00533
JACS Au 2023, 3, 293−305

from underground storage).[15] In this section, we describe tandem thermocatalytic−thermocatalytic and plasma-catalytic schemes for simultaneously upgrading CO_2 and ethane to C_3 Oxys.

2.1.1. Thermocatalytic−Thermocatalytic Scheme (TC-TC). In the TC-TC tandem reaction scheme, ethylene and syngas are first coproduced via CO_2-assisted oxidative dehydrogenation of ethane (CO_2−ODHE) and dry reforming of ethane (DRE), as shown in eqs R1 and R2, respectively.

$$C_2H_6 + CO_2 \rightarrow C_2H_4 + CO + H_2O \qquad \Delta G_{298K}{}^0 = +129.8\ \text{kJ/mol} \tag{R1}$$

$$C_2H_6 + 2CO_2 \rightarrow 4CO + 3H_2 \qquad \Delta G_{298K}{}^0 = +272.8\ \text{kJ/mol} \tag{R2}$$

Subsequently, ethylene and syngas are used as the reactants in the downstream hydroformylation reaction to produce propanal, as shown in eq R3; 1-propanol can also be produced by hydrogenation of propanal.

$$C_2H_4 + CO + H_2 \rightarrow C_2H_5CHO \qquad \Delta G_{298K}{}^0 = -57.4\ \text{kJ/mol} \tag{R3}$$

Figure 2 shows a thermodynamic analysis of relevant reactions at ambient pressure. As represented by the purple line, the direct one-step conversion of CO_2 and ethane to C_3 Oxys is thermodynamically unfavorable ($\Delta G^0 > 0$) across the entire temperature range. It is also evident that CO_2-ODHE (blue line)—which is the sum of the direct dehydrogenation of ethane (DDHE) and reverse water-gas shift (RWGS) reactions (black and green lines, respectively)—and DRE (red line) are favored at higher temperatures, while the hydroformylation reaction (gold line) is favored at lower temperatures.

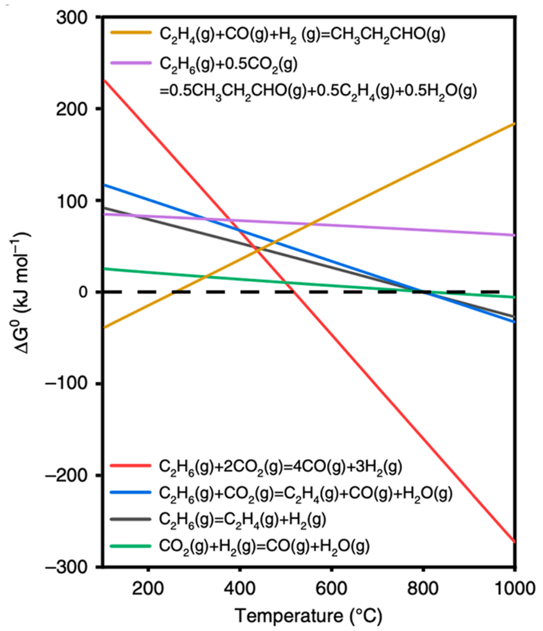

Figure 2. Diagram of standard Gibbs free energy change (ΔG^0) as a function of temperature for the relevant reactions of CO_2 and ethane. Reprinted with permission from Xie et al.[9] This work is licensed under a Creative Commons Attribution 4.0 International License (https://creativecommons.org/licenses/by/4.0/).

Therefore, a two-step tandem approach with CO_2-ODHE&-DRE and hydroformylation reactors operating within their respective favorable temperature regimes can bridge this temperature gap.

In comparison with the nonoxidative DDHE process, CO_2-ODHE favors coke elimination (via the reverse Boudouard reaction: $CO_2 + C \rightarrow 2CO$) and forward-shifts the reaction (via the RWGS reaction: $CO_2 + H_2 \rightarrow CO + H_2O$).[16−18] The use of CO_2 as a soft oxidant, as opposed to O_2, also mitigates overoxidation of hydrocarbons as well as the safety issues associated with the strongly exothermic O_2-assisted dehydrogenation (O_2-ODHE).[19] By tuning the relative contributions of the CO_2-ODHE and DRE reactions, the optimal mixture of C_2H_4, CO, and H_2 can be produced and fed to the downstream hydroformylation reactor. However, the DRE reaction typically outperforms the CO_2-ODHE reaction, as cleavage of the ethane C−C bond (368 kJ mol^{-1}) is more thermodynamically favorable than C−H bond scission (415 kJ mol^{-1}); thus, it remains challenging to enhance ethylene selectivity. Using a nonprecious Fe_3Ni_1/CeO_2 bimetallic catalyst, Xie et al. observed much lower C_2H_4 production relative to syngas production below 700 °C; however, incorporating the homogeneous contribution to ethylene production at 750 °C and above, the $C_2H_4/CO/H_2$ product ratio was similar to the 1/1/1 stoichiometric feed ratio required for the hydroformylation reaction (Figure 3a).[9]

For the conventional homogeneous hydroformylation of ethylene, high pressures are typically required in order to increase the concentration of reactants (i.e., olefins, CO, and H_2) in the solvent. Industrial phosphine-modified rhodium (Rh) catalysts have demonstrated very high activities (i.e., turnover frequencies up to 600 min^{-1} for α-olefins) with very low byproduct formation and alkene isomerization.[20] However, the homogeneous process deals with separation challenges, which may lead to precious-metal leaching and the generation of phosphorus-containing waste.[21] In contrast, in the heterogeneous hydroformylation of ethylene, an appreciable surface coverage of such reactants can be obtained over oxide-supported metal catalysts,[22−25] thereby allowing for reduced reaction pressures. As a result, heterogeneous supported metal catalysts can even be used at ambient pressure, as opposed to the typical homogeneous ligand-modified metal complexes used in industrial practice.[6] In general, unmodified Rh metal is more active than other monometallic catalysts and enables the hydroformylation reaction under milder conditions. Liu et al. summarized the performance of various heterogeneous Rh-based hydroformylation catalysts, including the use of organic phosphines, inorganic phosphides, and second metal modifications.[25]

As shown in Figure 3b, Xie et al. demonstrated that increasing the Co/Rh ratio in a RhCo bimetallic catalyst increased the C_3 Oxy yield as well as the alcohol/aldehyde product ratio.[9] The presence of Co was found to increase Rh particle dispersion and favor hydrogenation to 1-propanol, due to the stronger binding of key oxygenate intermediates ($*CH_3CH_2CHO$ and $*CH_3CH_2CH_2O$) on the RhCo bimetallic surface compared to the pure Rh surface, based on DFT calculations.[9] In the directly coupled tandem TC-TC configuration, the highest ethane-based yield of C_3 Oxys (4.7%) was obtained with Fe_3Ni_1/CeO_2 at 800 °C in the first reactor and Rh_1Co_3/MCM-41 at 200 °C in the second reactor (Figure 3c).[9] As expected, higher temperatures in the first CO_2-ODHE/DRE reactor and a higher Co/Rh ratio in the

https://doi.org/10.1021/jacsau.2c00533
JACS Au 2023, 3, 293−305

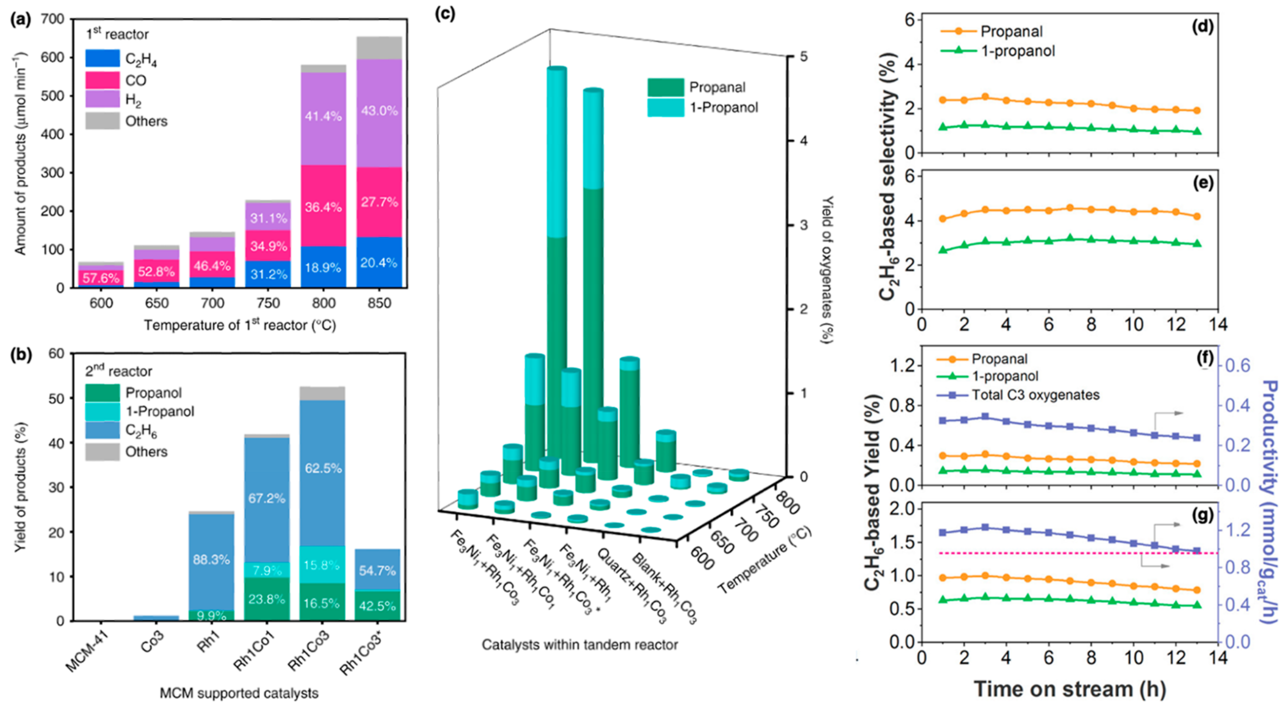

Figure 3. TC-TC tandem performance. (a) Amount of products formed during the first reaction step of CO_2 and C_2H_6 over a Fe_3Ni_1/CeO_2 catalyst at different temperatures. (b) C_2H_4-based product yields in a second reactor over the MCM-41-supported $RhCo_x$ catalysts at 200 °C. The values within the bars of Figure 3a,b indicate product selectivity. (c) C_2H_6-based yield in the tandem configuration (first reactor, 600−800 °C, Fe_3Ni_1/CeO_2 catalyst; second reactor, 200 °C, $RhCo_x$ catalysts). Reprinted with permission from Xie et al.[9] This work is licensed under a Creative Commons Attribution 4.0 International License (https://creativecommons.org/licenses/by/4.0/). (d, e) C_2H_6-based selectivity, and (f, g) C_2H_6-based yield and productivity for the tandem reactor system with reduced temperatures in the first reactor (first reactor, 550−600 °C, $PtSn_3/\gamma$-Al_2O_3 catalyst; second reactor, 200 °C, $RhCo_3$ catalyst). The upper and lower panels in Figure 3d−g represent the results obtained for the first reactor at 550 and 600 °C, respectively. The pink dashed line in Figure 3g indicates the productivity of total C_3 oxygenates obtained in the tandem system containing the Fe_3Ni_1/CeO_2 catalyst at 750 °C. Reprinted with permission from Xie et al.[10] Copyright 2022, American Chemical Society.

second hydroformylation reactor led to the optimal production of C_3 Oxys.

With the homogeneous contribution to ethylene formation at high temperatures, the control over selectivity was compromised. Thus, it is critical to reduce the temperature in the first reactor to enable a completely catalytic tandem process, in which the $C_2H_4/CO/H_2$ ratios can be better tuned via the selection of appropriate catalysts. Xie et al. recently analyzed and identified the desired $C_2H_4/CO/H_2$ ratios by considering different combinations of main and side reactions of CO_2 and ethane.[10] To obtain a $C_2H_4/CO/H_2$ ratio that is close to the typical feed ratio (1/1/1) for the subsequent hydroformylation, the analysis showed that the desired catalysts for the first reactor should enable multiple simultaneous reactions of direct dehydrogenation of ethane (DDHE), ODHE, DRE, and RWGS: i.e., either ODHE + DDHE + DRE (theoretical product ratio of 1/1/0.88) or DDHE + RWGS + DRE (theoretical product ratio of 1/1.15/1). Accordingly, a typical dehydrogenation catalyst, i.e., $PtSn_3/\gamma$-Al_2O_3, was identified to be promising to promote the simultaneous DDHE (major), ODHE (minor), and DRE reactions at a lower temperature (i.e., 550−600 °C) and, in turn, supply a mixture of C_2H_4, CO, and H_2 (1/0.9/0.4) for the second reactor (Figure 3d−g). It should be noted that the stoichiometric ratio (1/1/1) is a typical benchmark for single-site catalysts (e.g., $RhCo_x$/MCM-41 in Figure 3) in conventional hydroformylation processes. Yet, the preferred ratio could be different in the case of catalysts with bifunctional active sites, as demonstrated by the recently reported Rh-WO_x pair sites, where a higher fraction (or partial pressure) of CO is favorable for propanal formation.[24] In the tandem configuration with $PtSn_3/\gamma$-Al_2O_3 catalyst at 600 °C in the first reactor, the obtained C_3 Oxy productivity was comparable to that of the aforementioned Fe_3Ni_1/CeO_2 catalyst at 750 °C (Figure 3g).[10]

2.1.2. Plasma−Thermocatalytic Scheme (P-TC). As shown in the thermodynamic analysis in Figure 2, the one-step conversion of CO_2 and ethane to C_3 Oxys is not feasible; a gap exists between the high temperatures required to activate the stable C═O and C−H bonds and the low temperatures that favor the exothermic oxygenate production. Instead of using a two-step TC-TC approach, however, nonthermal plasma can be used to overcome the thermodynamic limitations and produce C_3 Oxys in one step under mild conditions. In nonthermal plasma, a large voltage difference between two electrodes is used to activate the gaseous reactants and form a nonequilibrium phase containing electrons, ions, radicals, atoms, molecules, and other excited species, which can subsequently react and recombine into desirable products. Despite the bulk gas remaining at or near ambient conditions, the highly energized electrons (typically 1−10 eV) within the plasma can overcome the energy barriers associated with chemical ionization and bond dissociation (i.e., E_{diss} = 4.4 eV for C═O, E_{diss} = 5.5 eV for C−H).[26] Plasma also offers other distinct advantages over thermocatalytic processes, including fast reaction rates that allow for rapid process startup/shutdown and easier integration with intermittent renewable electricity sources.[27]

https://doi.org/10.1021/jacsau.2c00533
JACS Au 2023, 3, 293−305

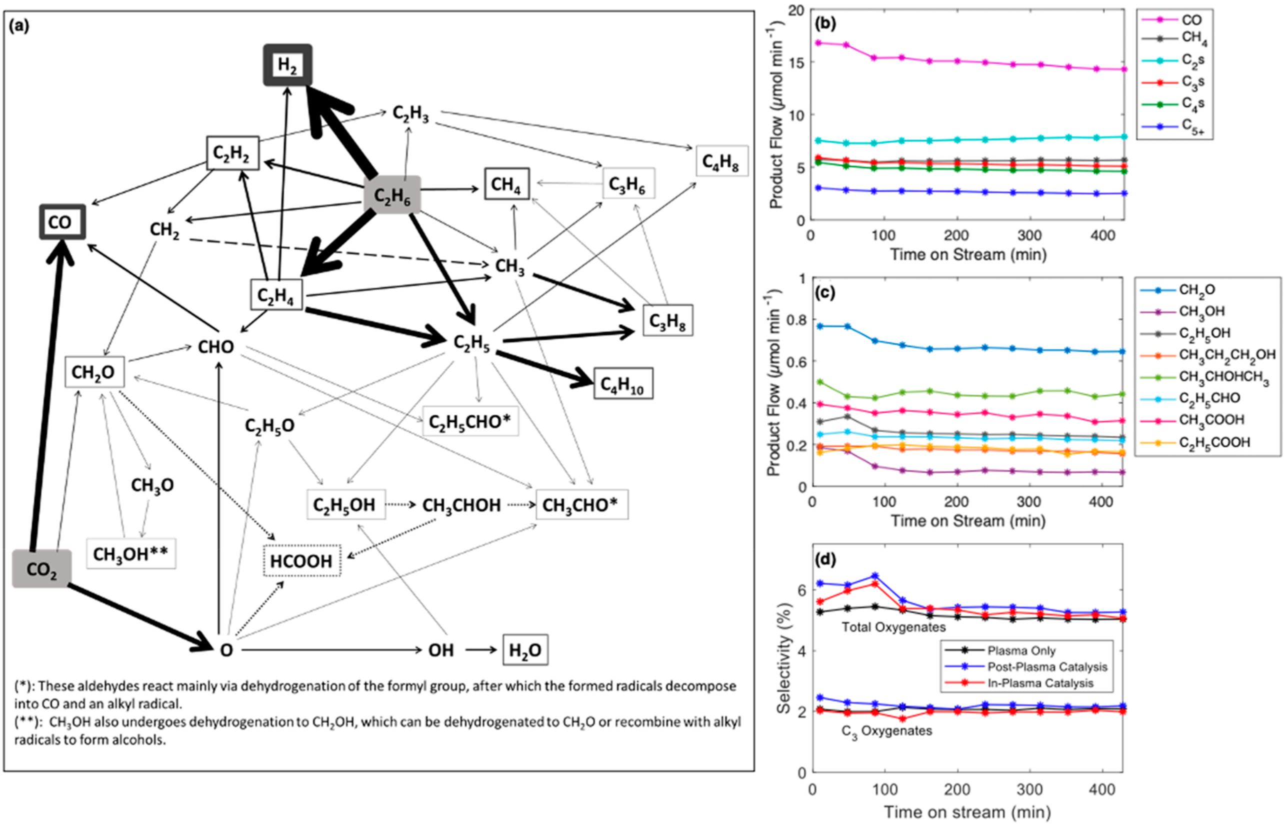

Figure 4. P-TC tandem performance. (a) Schematic of the most important CO_2 + ethane plasma reaction pathways, where the thickness of arrows and frames indicates the relative importance of the corresponding pathways and product densities, respectively. Dotted lines indicate very low rates and densities. (b) Flow rates of CO and hydrocarbon products and (c) flow rates of oxygenate products for the plasma-only reaction of CO_2 and ethane at 10.0 kV and 9 kHz under ambient pressure and 200 °C. (d) Effect of adding $RhCo_3$/MCM-41 catalyst on oxygenate selectivity. Reprinted with permission from Biswas et al.[11] Copyright 2022, American Chemical Society.

Plasma-activated reactions between CO_2 and ethane have been demonstrated to generate C_3 Oxys.[11] The complexity of the production and destruction pathways occurring within the plasma (Figure 4a) has been described for the full list of reactions as determined by plasma chemical kinetic modeling by Biswas et al.[11] The formation of C_3 Oxys, among other products, from a plasma-activated reaction of CO_2 and ethane was achieved using a dielectric barrier discharge (DBD) reactor at atmospheric pressure and 200 °C. In addition to CO and C_1−C_{5+} hydrocarbons, a variety of oxygenate products were generated, including formaldehyde, acetic acid, methanol, ethanol, 1-propanol, 2-propanol, and propanal (Figure 4b,c). Increasing the plasma power was found to increase CO_2 and ethane reactant conversions, but higher total oxygenate selectivities were obtained at lower powers. Additionally, a greater CO_2/ethane feed ratio reduced the formation of hydrocarbons in favor of CO and oxygenated species, with a maximum oxygenate selectivity of 12% obtained at a 4/1 CO_2/ethane feed ratio.

The primary issue limiting the plasma-only reaction of CO_2 and ethane is low product selectivity. The highest C_3 Oxy selectivity achieved by Biswas et al. was 2.9%,[11] necessitating energy-intensive separations to isolate these products from the numerous other oxygenate and hydrocarbon species generated. One possible approach to improving selectivity involves coupling the plasma-activated reaction with suitable thermo-catalysts. Catalysts can be placed within the plasma zone to interact with short-lived plasma species (such as ions, radicals, and vibrationally excited molecules) or downstream of the plasma zone where long-lived quasi-stable intermediates can reach the catalyst bed. Given the formation of ethylene and syngas in the plasma-activated reaction, the heterogeneous Rh_1Co_3/MCM-41 hydroformylation catalyst (as discussed in section 2.1.1) was initially considered to be a promising candidate to enhance C_3 Oxy production. However, Biswas et al. found the inclusion of Rh_1Co_3/MCM-41 only increased total oxygenate selectivity at early time scales (<100 min of time on stream) and had a negligible effect on the C_3 Oxy production (Figure 4d). Instead, the formation of formaldehyde and acids was favored, indicating that the presence of a catalyst altered the reaction pathways and product distribution.[11] The desired catalytic effect to enhance C_3 Oxy production may not have been observed if excess H_2 promoted ethylene hydrogenation more than the hydroformylation reaction. Additionally, the lack of catalytic effect may also be related to material shielding effects, where the plasma discharge may be unable to penetrate into the mesopores of the porous support (i.e., MCM-41) where the active catalyst metals were deposited.[28] The plasma-activated conversion of CO_2 and ethane was also investigated by Gomez-Ramirez et al.[29] While formaldehyde was the only oxygenate product detected, the incorporation of a vanadia/alumina catalyst dispersed on a $BaTiO_3$ ferroelectric was found to significantly enhance formaldehyde production, further demonstrating the possibilities for combining catalysts with plasma excitations to modify the product selectivity.

https://doi.org/10.1021/jacsau.2c00533
JACS Au 2023, 3, 293−305

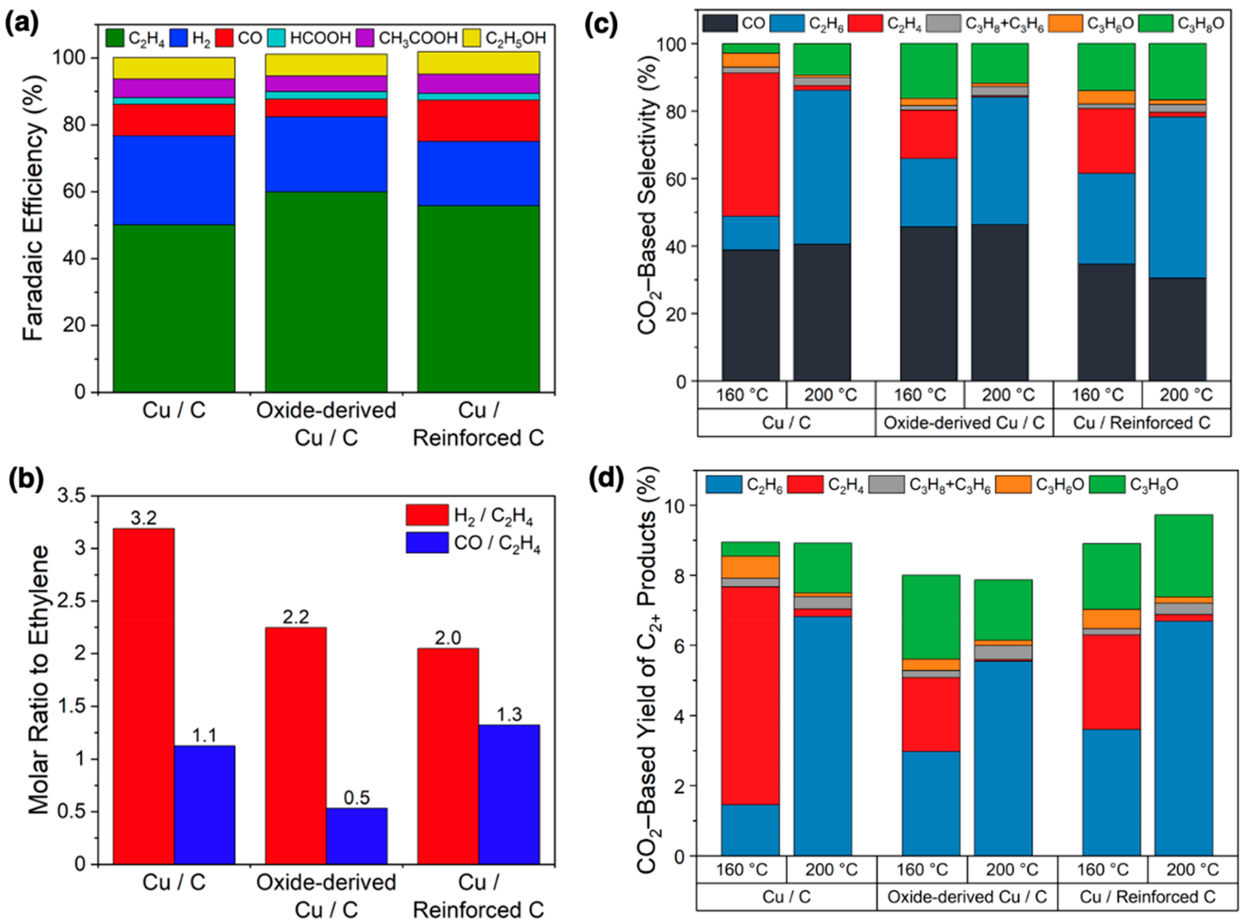

Figure 5. EC-TC tandem performance. (a) Faradaic efficiencies for CO_2RR on commercial Cu on carbon, oxide-derived Cu on carbon, and Cu on reinforced carbon GDL at −220 mA cm^{-2}. (b) Electrochemical product selectivity represented in terms of relative molar ratios. (c) CO_2-based selectivities and (d) yields of products in the tandem configuration for Cu/C, oxide-derived Cu/C, and Cu/reinforced C cathodes at −220 mA cm^{-2} in combination with 160 and 200 °C hydroformylation temperatures. Reprinted with permission from Biswas et al.[12] Copyright 2022, American Chemical Society.

2.2. Upgrading CO_2 with H_2O

The electrocatalytic conversion of CO_2 to C_3 Oxys with water as the hydrogen source is an alternative to the ethane-based thermocatalytic and plasma-catalytic processes. Electrochemical processes are often advantageous because of their operation under ambient temperature and pressure, scalability, and ease of integration with renewable electricity sources. When it is employed for CO_2 conversion, water is often introduced in the form of a humidified CO_2 feed and/or an aqueous electrolyte solution (e.g., H_2O, $KHCO_3$, KOH) in low-temperature electrolysis. Unlike the temperature-gap limitations in the thermochemical CO_2 + ethane reactions, CO_2 can be electrochemically reduced to C_3 Oxys in one step. However, due to the large overpotentials and multitude of competing reactions, the direct CO_2 reduction to 1-propanol in flow cells has only been demonstrated with very low selectivities, limited to Faradaic efficiencies (FEs) of <5%.[30,31] Furthermore, the separation of C_3 Oxys from other dilute liquid products (such as formic acid, acetic acid, and ethanol) within an aqueous electrolyte is challenging and energy-intensive. Instead, a two-step tandem approach can break down the process into simpler components and improve the overall energy efficiency and C_3 Oxy production rate. In this section, we discuss the tandem electrocatalytic−thermocatalytic and electrocatalytic−electrocatalytic schemes for CO_2 conversion to C_3 Oxys using water as the hydrogen source.

2.2.1. Electrocatalytic−Thermocatalytic Scheme (EC-TC). In the EC-TC tandem reaction scheme, the first reactor step of the TC-TC process involving CO_2-ODHE and DRE reactions (eqs R1 and R2, respectively) is replaced with the electrochemical CO_2 reduction reaction (CO_2RR) to produce C_2H_4 and CO (eqs R4 and R5, respectively) and the hydrogen evolution reaction (HER) to produce H_2 (eq R6). The products of these electrochemical reactions, C_2H_4 and syngas, are then directly fed as the reactants to a downstream thermochemical heterogeneous hydroformylation reactor (eq R3), as in the second step of the TC-TC scheme.

$$2CO_2 + 12H^+ + 12e^- \rightarrow C_2H_4 + 4H_2O \quad E^0 = 0.08 \text{ V vs RHE} \tag{R4}$$

$$CO_2 + 2H^+ + 2e^- \rightarrow CO + H_2O \quad E^0 = -0.10 \text{ V vs RHE} \tag{R5}$$

$$2H^+ + 2e^- \rightarrow H_2 \quad E^0 = 0 \text{ V vs RHE} \tag{R6}$$

These three reactions are typically considered to be problematic competing reactions, and most electrocatalytic research has traditionally focused on minimizing side reactions

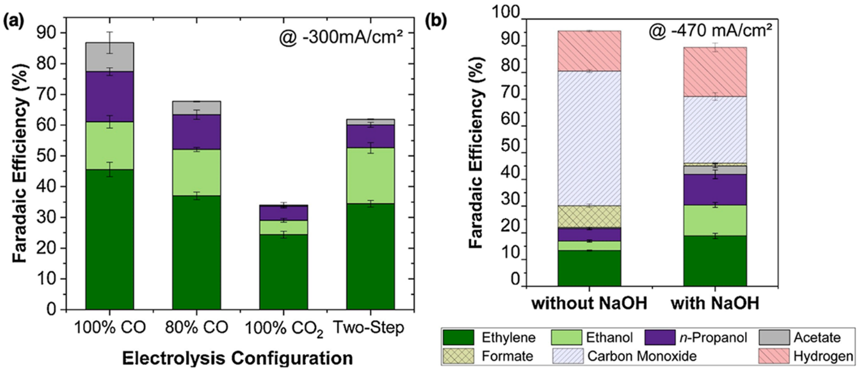

Figure 6. EC-EC tandem performance. (a) Cumulative Faradaic efficiencies at a current density of −300 mA cm^{-2} from single-step electrolysis with pure CO, an 80% CO/20% CO_2 mixture, and pure CO_2 compared to the two-step tandem configuration. (b) Faradaic efficiencies in the tandem configuration at −470 mA cm^{-2} with and without the NaOH absorber. Reprinted with permission from Romero Cuellar et al.[13] Copyright 2020, Elsevier.

in favor of producing a single desired species. In particular, suppressing excess H_2 formation via the HER remains a challenge due to the presence of water-based electrolytes and the highly negative overpotentials required to drive the CO_2RR. Despite this issue, several recent studies have demonstrated the selective production of C_2H_4, with FEs as high as 83%.[32−34] In contrast, the EC-TC approach seeks to leverage these competing reactions in order to coproduce C_2H_4, CO, and H_2 to be used directly as the feed for the subsequent thermocatalytic hydroformylation reaction.

Due to its intermediate binding energies of H* and CO*, copper (Cu) is the only monometallic catalyst that is able to electrochemically convert CO_2 into C_2H_4, as well as any other product with more than two electron transfers.[35,36] Extensive research has been conducted on the CO_2RR over Cu electrocatalysts, including the effects of surface structure, morphology, composition, electrolyte, pH, and cell design, as summarized in a comprehensive review by Nitopi et al.[37] In a demonstration of the tandem EC-TC system, Biswas et al. used Cu nanoparticle electrocatalysts with different oxidation states (i.e., Cu and oxide-derived Cu catalysts), as well as modifications to the gas diffusion layer (GDL) hydrophobicity (i.e., fluorinated ethylene propylene (FEP) reinforced carbon) in a zero-gap, vapor-fed flow electrolyzer with a Sustainion anion exchange membrane.[12] Relative to the benchmark Cu on carbon GDL, the oxide-derived Cu and FEP-reinforced carbon GDL cathodes enhanced the ethylene FE from 50% to 60% and lowered the H_2 FE from 27% to 19% at a cell current of −220 mA cm^{-2}, as shown in Figure 5a. The FE values describe the distribution of charge transferred and are not directly comparable to the thermocatalytic definition of selectivity; therefore, the relative molar production rates are also presented in Figure 5b. The C_2H_4/CO/H_2 product ratios obtained from the electrolyzer were 1/1.1/3.2 (for Cu/C), 1/0.5/2.2 (for oxide-derived Cu/C), and 1/1.3/2.0 (for Cu/FEP-reinforced C), which were then fed to the thermocatalytic hydroformylation reactor.

Biswas et al. used the same Rh_1Co_3/MCM-41 hydroformylation catalyst in the EC-TC system as was previously employed in the TC-TC and P-TC schemes.[12] In the directly coupled tandem configuration, the highest C_3 Oxy selectivities obtained were 18.4% for the oxide-derived Cu/C electrode coupled with a 160 °C hydroformylation temperature and 18.0% for the Cu/FEP-reinforced C electrode coupled with a 200 °C hydroformylation temperature (Figure 5c), which corresponded to C_3 Oxy yields of 2.7% and 2.5%, respectively (Figure 5d). The remainder of the carbon-containing products consisted primarily of CO and ethylene (CO_2RR products that were unconverted in the thermocatalytic reactor) or ethane (undesired product from C_2H_4 hydrogenation), which further highlights the need for inhibiting the HER in the upstream CO_2 electrolyzer and developing more active and selective hydroformylation thermocatalysts.

2.2.2. Electrocatalytic−Electrocatalytic Scheme (EC-EC). As discussed above, the direct electrochemical conversion of CO_2 to multicarbon products (such as ethylene, ethanol, and 1-propanol) remains challenging due to low selectivities and high overpotentials. It has been well-established, however, that CO is the key reaction intermediate during the CO_2RR to C_{2+} species over Cu electrodes.[38] Therefore, feeding pure CO can enable an increased surface coverage of CO and C−C coupling and consequently enhance C_{2+} product formation.[39] As a result, CO_2 electrolysis can be conducted in a tandem EC-EC scheme, in which CO_2 is first electrochemically reduced to CO (eq R5), followed by the CO reduction reaction (CORR) to propanol, as shown in eq R9.

$$3CO + 12H^+ + 12e^- \rightarrow C_3H_7OH + 2H_2O$$
$$E^0 = 0.20 \text{ V vs RHE} \quad \text{(R9)}$$

For CO_2-to-CO electrolysis, a variety of catalytic materials, including precious and earth-abundant metals, transition-metal chalcogenides, and carbon-based catalysts, have effectively converted CO_2 to CO, with FEs reaching >95%.[40] Additionally, several studies have reported CO electrolysis to C_{2+} products over Cu-based catalysts with high FEs (>75%) at current densities of up to 1 A cm^{-2},[41−43] representing a significant performance improvement over the CO_2RR.[44−46] At present, tandem CO_2/CO electrolysis strategies have primarily demonstrated enhanced production of acetate, ethylene, and ethanol,[47−50] including the development of tandem catalyst architectures within a single device.[51−53] However, the focus of the current Perspective is mainly on the implementation of a two-step EC-EC system that produced C_3 Oxys.

Romero Cuellar et al. used two flow electrolyzers in series, with an Ag gas diffusion electrode in the first electrolyzer and Cu nanoparticles on a carbon-based gas diffusion electrode in the second electrolyzer.[13] Although >90% FE to CO was obtained in the first electrolyzer, the outlet contained large

https://doi.org/10.1021/jacsau.2c00533
JACS Au 2023, 3, 293−305

amounts of unconverted CO_2. Therefore, the CO_2 feed rate and applied voltage had to be carefully controlled in order to maximize CO_2 conversion without compromising CO selectivity relative to the competing HER. The second CO electrolyzer was then tested with varying CO/CO_2 feed ratios to simulate the outlet from the upstream reaction. As shown in Figure 6a, a larger CO/CO_2 feed ratio resulted in an enhanced production of 1-propanol and C_2 products, again illustrating the clear advantage of the CORR to multicarbon products versus the CO_2RR.

Due to the observed benefits of feeding pure CO to the second electrolyzer, Romero Cuellar et al. also integrated a CO_2 absorption column filled with 5 M NaOH between the two electrolyzers.[13] While the NaOH absorber purified the CO feed and enhanced the overall selectivity to C_{2+} products (Figure 6b), it also sacrificed CO_2 conversion and would require additional energy input to recover the captured CO_2. Improving CO_2 single-pass conversion would minimize the energy costs of separating unreacted CO_2 and potentially eliminate the need for any intermediate separation altogether. With the coupled electrolyzers (-100 mA cm^{-2} in the first cell, -200 mA cm^{-2} in the second cell) along with the NaOH separation step, Romero Cuellar et al. achieved a combined FE of 62% for C_{2+} products, including 7.5% FE to 1-propanol.[13] It is important to note that this work was not specifically aimed at maximizing 1-propanol production. Therefore, more targeted electrocatalysts that have previously been shown to favor the CORR to 1-propanol could improve the overall tandem performance for C_3 Oxy production.[54−56]

3. COMPARISON OF ENERGY COSTS AND PROSPECTS FOR NET CO_2 REDUCTION

Valuable C_3 Oxys may be produced more sustainably using the alternative ambient-pressure tandem processes described above, by reacting CO_2 either with surplus ethane in underutilized shale gas fractions via TC-TC or P-TC schemes or with water via EC-TC and EC-EC schemes. Evaluating these alternative approaches requires comparing their energy costs and prospects for achieving a net consumption of CO_2, but it is difficult to directly compare the various tandem strategies due to discrepancies in the as-published results. For instance, electrocatalytic studies typically report Faradaic efficiencies and partial current densities (and infrequently CO_2 conversions), while thermocatalytic studies report conversions, selectivities, and yields. Moreover, even within the thermocatalysis literature, there are often inconsistencies in how these metrics are defined. Comparing across these metrics is even more challenging in tandem reaction schemes, in which different types of reactors are combined in series. Therefore, in order to provide a fair comparison, we calculate the C_3 Oxy yield on a CO_2 basis using the equation

$$\text{yield} = \frac{F_{\mathrm{C_3Oxy,out}}}{F_{\mathrm{CO_2,in}}} \times \frac{n_{\text{carbon atoms from CO}_2\text{ in C}_3\text{Oxy}}}{n_{\text{carbon atoms in CO}_2}} \times 100\% \quad (1)$$

where $F_{\mathrm{C_3Oxy,out}}$ is the total C_3 Oxy formation rate and $F_{\mathrm{CO_2,in}}$ is the CO_2 feed rate. The number of carbon atoms from CO_2 in C_3 Oxys equals 3 for the CO_2 + H_2O schemes (since CO_2 is the only carbon source) and 1 for the CO_2 + ethane schemes (since the remaining 2 carbon atoms are derived from ethane). We note that the exact number of carbon atoms from CO_2 may be different for the plasma-activated reaction due to more complex reaction pathways. The tandem C_3 Oxy production rates are either directly taken from the results cited above or back-calculated from reported conversions and selectivities (or currents and FEs), as summarized in Table S1. In addition, the energy input per mole of C_3 Oxys produced is calculated based on the driving force of each reaction type: i.e., temperature for thermochemistry and electrical energy for electrochemistry and plasma.

Figure 7a shows a comparison of the yields and energy costs of the laboratory-scale tandem schemes reported in the literature (see the Supporting Information for calculation details). In this comparison, we include the state-of-the-art demonstrated tandem results with the largest C_3 Oxy yields and lowest energy costs per mole of C_3 Oxy produced. The TC-TC scheme demonstrated the highest C_3 Oxy yield of 6.3%, while the P-TC scheme had the lowest yield of 0.4%. The higher yields of the TC-TC approach are consistent with the issues associated with CO_2 loss (and hence, low conversion) in the electrochemical-based systems and the low selectivity of the plasma-activated reaction. The EC-TC scheme has the lowest energy cost per mole of C_3 Oxy, as a result of replacing the high-temperature CO_2-ODHE/DRE thermocatalytic reactor step with CO_2 electrolysis at ambient temperature. The EC-TC system also utilizes a low-temperature hydroformylation reactor in the second step as opposed to the more difficult electrochemical conversion of CO/CO_2 to C_3 Oxy products. The energy cost in the P-TC scheme is especially high, due to the large power input in combination with the low C_3 Oxy production rate.

Any viable CO_2 utilization technology must consume more CO_2 than the process emits, or at a minimum, emit less CO_2 than the conventional process it replaces. Therefore, it is essential to consider the CO_2 emissions associated with these tandem processes, where the energy input typically accounts for the majority of the CO_2 footprint. Figure 7b plots the net CO_2 emissions per mole of C_3 Oxy produced as a function of the CO_2 emissions per unit energy for the four tandem reaction strategies (see the Supporting Information for more details regarding emissions calculations). Based on the currently demonstrated laboratory-scale results, the net CO_2 emissions are largely positive and in the trend of EC-TC < TC-TC < EC-EC < P-TC, following the trends in energy cost per mole of C_3 Oxy produced. As we shift from the average CO_2 emissions associated with the U.S. grid electricity (~0.39 kg-CO_2/kWh)[57] to less carbon-intensive energy sources (i.e., moving leftwards on the x axis), the overall net CO_2 emissions can be reduced. Unsurprisingly, net negative emissions can only be realized for any of the laboratory-scale processes if a significant portion of the energy input is obtained from renewable sources (<0.06 kg-CO_2/kWh). Therefore, compatibility with renewable energy must be a key consideration in the potential commercial-scale implementation of any tandem CO_2 conversion strategy. With completely carbon-free energy (i.e., 0 kg-CO_2/kWh), the EC-EC and EC-TC schemes can theoretically reduce 3 mol of CO_2 into 1 mol of C_3 Oxy, while the TC-TC and P-TC schemes only reduce 1 mol of CO_2 into 1 mol of C_3 Oxy due to the carbon contribution from ethane.

Based on Figure 7a,b using the currently available experimental results, all of the tandem processes have a greater energy cost and CO_2 footprint than those of the existing 1-propanol production process (energy cost of ~1.32 kWh/mol-C_3 Oxy; CO_2 footprint of ~4.23 mol-CO_2/mol-C_3 Oxy).[58] Therefore, the conventional 1-propanol production process is

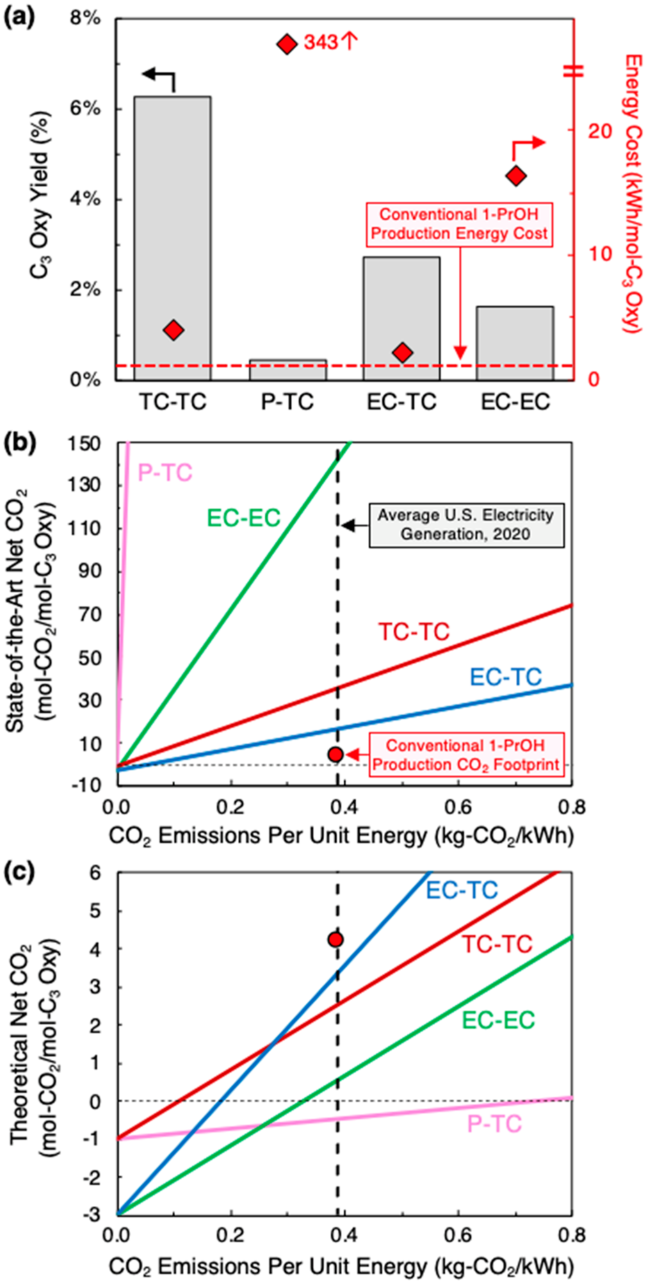

Figure 7. Comparison of energy costs and net CO_2 emissions of the alternative ambient-pressure tandem schemes for the production of C_3 oxygenated hydrocarbons (C_3 Oxys). (a) C_3 Oxy yields (left) and energy costs per mole of C_3 Oxy produced (right) for each of the tandem schemes. The red dashed line represents the energy cost for conventional 1-propanol production. (b) Net CO_2 emissions as a function of CO_2 emissions per unit energy based on demonstrated laboratory-scale results. (c) Theoretical net CO_2 emissions calculated for the ideal scenarios based on minimum energy requirements. In (b) and (c), the vertical black dashed line represents the average CO_2 emissions associated with U.S. grid electricity and the red data point represents the CO_2 footprint for conventional propanol production.

unlikely to be replaced by the state-of-the-art tandem schemes without an improvement in catalytic performance and/or utilization of low-carbon energy sources. It should also be noted that the calculations in Figure 7a,b were performed based on currently demonstrated laboratory-scale results, since none of the tandem processes have been implemented at scale and therefore reliable parameters for plant-level process simulation are unavailable. As a result, the analysis for the tandem schemes does not consider the CO_2 emissions associated with obtaining feedstocks: namely, CO_2 capture, ethane extraction and separation, and water purification. Energy savings via heat integration were also not accounted for in the energy cost calculations (e.g., heat integrating the first endothermic reactor and second exothermic reactor in the TC-TC scheme).

Moreover, downstream separation processes were not considered, although these may ultimately constitute a large fraction of the process energy consumption depending on the final C_3 Oxy concentration supplied by the tandem reactors. Among the four tandem processes, the TC-TC and EC-TC tandem schemes would likely have significant separation advantages due to the ease of separating targeted liquid oxygenates from the gaseous outlet stream of a thermocatalytic reactor. Both TC-TC and EC-TC should have similar separations following the hydroformylation reactor; however, the EC-TC scheme may have additional water content originating from the electrolyte in the upstream electrolyzer. In contrast, P-TC (which produces a wide range of liquid products) and EC-EC (which requires liquid–liquid separation of dilute products from an aqueous electrolyte) would likely involve much more energy-intensive separations.

Although the results presented in this Perspective serve as a useful proof of concept, they remain far from optimized. Therefore, in Figure 7c, we include a comparison of net CO_2 emissions as calculated from theoretical limits, thus representing an upper bound for performance. As given in Table S2, the minimum energy requirements were determined from the enthalpy of reactions for thermochemistry, reversible cell potentials for electrochemistry, and vibrational excitation energies for plasma chemistry and by assuming the absence of any competing reactions. More details regarding the theoretical minimum energy calculations are provided in the Supporting Information. Although these assumptions are highly optimistic, this method allows for a comparison of the best-case scenarios. Figure 7c shows a trend of P-TC > EC-EC > EC-TC > TC-TC based on the crossover points for reaching net negative emissions. Even though the P-TC and TC-TC pathways have a lower thermodynamic energy requirement, the electrocatalytic-based tandem schemes have the advantage of converting 3 mol of CO_2 into C_3 Oxys. More importantly, for all four tandem strategies, there are significant opportunities for reducing energy input and CO_2 emissions relative to the currently demonstrated performance. Future advances in catalyst development and reactor design will enable progress toward these theoretical limits. Engineering optimizations, such as heat integration and reactant recycling, can also help minimize energy costs and thereby reduce CO_2 emissions.

4. CHALLENGES AND OPPORTUNITIES

In this Perspective, we present four tandem reaction strategies, TC-TC, P-TC, EC-TC, and EC-EC, to produce C_3 Oxys using CO_2 as a reactant at atmospheric pressure. The tandem catalytic strategies may be a promising approach to reducing atmospheric CO_2 concentrations while simultaneously producing high-value C_3 oxygenates. However, these tandem schemes have been reported in the literature only as proof-of-concept demonstrations; thus, opportunities to improve and optimize these processes are significant. Currently, these systems operate far from the theoretical limits shown in

Figure 7c and will require significant improvements before becoming competitive with existing C_3 Oxy synthesis methods. We summarize the main challenges and opportunities for tandem reactions in this section.

4.1. Thermocatalytic Schemes

A major challenge for the tandem TC-TC and EC-TC schemes is the development of efficient heterogeneous hydroformylation catalysts to increase the C_3 Oxy selectivity relative to ethane, which is produced via the competitive ethylene hydrogenation reaction. As shown in Figures 3b and 5c,d, ethane is often observed to be the primary product. This can be attributed to the common C_2H_5* intermediate involved in the competing reaction pathways, which can more easily undergo hydrogenation than CO insertion—the typical rate-determining step of hydroformylation. Moreover, strong CO binding leads to significant competition with ethylene over single active sites, as suggested by the negative reaction order with respect to the CO partial pressure.[22] Thus, a selective hydroformylation catalyst should favor ethylene adsorption and CO insertion while making H_2 activation kinetically slower, which can be achieved via bifunctional active sites.[24] For example, the recently reported Rh-WO_x pair sites by Ro et al. were demonstrated to (1) facilitate W^{6+} reduction to form the active Rh−W site, (2) alleviate the typical CO poisoning effect by transferring adsorbed C_2H_4 from W to Rh, and (3) promote CO insertion and propanal formation via H_2 activation at the Rh−W interface to form a bridging hydride that facilitates adsorption of a third CO on Rh before acylation.[24] The pair sites exhibited extremely high selectivity (>95%) and production rate (0.1 g cm^{-3} h^{-1}) of propanal in heterogeneous ethylene hydroformylation. Therefore, the employment of bifunctional active sites with facile site cooperation during the catalytic cycle is an important approach to circumventing the undesired ethylene hydrogenation. In a practical system, the ethane byproduct can be easily separated from the liquid C_3 Oxy products and recycled as a reactant to the first reactor, reducing the natural-gas-derived ethane feed requirement and increasing the overall conversion efficiency.

4.2. Electrocatalytic Schemes

Suppressing the overproduction of H_2 via the HER remains a key challenge in aqueous-based electrochemical systems. This is especially relevant in the EC-TC scheme, where the excessive production of H_2 (e.g., H_2/C_2H_4 ratio >2 as shown in Figure 5c) promotes undesired ethylene hydrogenation over hydroformylation in the downstream thermocatalytic reactor. Various strategies, including the use of nanostructured catalysts, highly alkaline electrolytes, ionic liquids, and hydrophobic additives, have shown promise in inhibiting HER kinetics; however, further systematic studies are required to tune the relative product ratios. Alternatively, high-temperature solid oxide electrolyzer cells (SOECs) may be employed to avoid liquid electrolytes altogether, where cofeeding varying amounts of steam can potentially enable better control over the H_2 production rates.

The low product yields in the EC-TC system were also attributed to large CO_2 losses to carbonate formation and crossover within the electrolyzer, representing another significant challenge for low-temperature CO_2 electrolysis.[59,60] Under the highly alkaline conditions near the electrode surface (due to the consumption of protons and the formation of equivalent amounts of OH^- in CO_2RR and HER), CO_2 can rapidly react with OH^- to produce (bi)carbonates, as shown in eqs R7 and R8.

$$OH^- + CO_2 \rightarrow HCO_3^- \quad (R7)$$

$$OH^- + HCO_3^- \rightarrow CO_3^{2-} + H_2O \quad (R8)$$

These (bi)carbonates either accumulate within the electrolyte or migrate across the anion exchange membrane, where they are protonated and released as CO_2. This issue is further exacerbated by the large overpotentials required for the CO_2RR to C_2H_4 that increase the OH^- concentration, as well as the excess CO_2 feed needed to support high current densities. Therefore, novel electrolyzer cell designs or strategies that can efficiently regenerate and recycle CO_2 should be employed to improve the overall carbon conversion to C_3 Oxys in the EC-TC tandem scheme.

While CO_2 losses also affect the performance of the CO_2RR step in the EC-EC scheme, these losses occur to a lesser extent than in the EC-TC scheme. The maximum carbon efficiency is 25% for CO_2-to-C_2H_4 electrolysis (three CO_2 molecules converted to carbonate per CO_2 to C_2H_4), whereas CO_2-to-CO has a maximum carbon efficiency of 50% (one CO_2 to carbonate per CO_2 to CO).[59] Despite the relative advantage of converting CO_2 to CO instead of C_2H_4, state-of-the-art low-temperature CO_2-to-CO flow electrolyzers have only demonstrated single-pass conversions of up to 33%.[61] Alternative cell configurations, such as the use of bipolar membranes (BPMs)[62−64] or SOECs,[65,66] can potentially circumvent issues with carbonate formation; however, their respective tradeoffs must also be considered (i.e., more negative overpotentials for water dissociation and lower CO FEs in BPMs and elevated operating temperatures in SOECs). Unlike CO_2RR, CO electrolysis can avoid CO_2 losses to carbonate and has demonstrated higher single-pass conversions.[67] However, previous experimental trends have shown 1-propanol selectivities to be inversely related to partial currents, with FEs dropping below 10% at partial current densities above 40 mA cm^{-2}.[44] More recently, though, Wang et al. reported 36% FE to 1-propanol at 300 mA cm^{-2} and 85% CO conversion with Ag−Ru−Cu catalysts, demonstrating the possibility for more active and selective electrocatalysts for C_3 Oxy production via the EC-EC scheme.[68]

4.3. Plasma-Catalytic Scheme

While the P-TC scheme can accomplish one-pot C_3 Oxys production, the high energy consumption and wide product distribution present significant challenges. Additional plasma-catalysis studies are essential to improve the selective conversion of CO_2 and ethane to C_3 Oxys. Although well-established protocols for product prediction and catalyst screening do not currently exist, inspiration can be drawn from the plasma-activated reaction between CO_2 and methane, in which DBD reactors packed with catalysts (e.g., reducible metal oxides and copper) and high-dielectric-constant additives (e.g., $BaTiO_3$) have been found to enhance the production of methanol and other oxygenates.[69] Furthermore, the use of plasma kinetic modeling can provide valuable insights into the dominant reaction pathways. For instance, Biswas et al. used plasma kinetic modeling, in combination with $^{12}CO_2/^{13}CO_2$ isotopic labeling experiments, to reveal a CO_2 + ethane plasma reaction mechanism that proceeded via oxidation of ethane-derived species by oxygen from CO_2, which is different from the thermocatalytic alcohol formation

https://doi.org/10.1021/jacsau.2c00533
JACS Au 2023, 3, 293−305

pathway that involves either CO_2 hydrogenation or CO insertion.[11] Therefore, catalysts that promote conventional thermochemical reaction pathways to oxygenates may not necessarily be the ideal candidates for the corresponding plasma-activated reactions. The effects of various catalysts and support materials on the plasma, and vice versa, should be further studied. Approaches that aim to tune both the plasma conditions as well as the catalytic surface reactions will likely be necessary to achieve sufficient control over product selectivity. However, for applications that require high-purity C_3 Oxys, plasma-catalytic schemes are unlikely to be competitive due to the energy-intensive postreaction separation steps that would be required to separate products with similar physicochemical properties, such as mixed alcohols or liquids with similar boiling points. Alternatively, plasma-catalytic schemes may be more appropriate for applications that can tolerate a wider distribution of products among the liquid fraction, such as blended alcohol or oxygenate product streams for fuel applications.

4.4. Future Directions

Although many research efforts have been dedicated to the individual reaction steps, more systematic studies should be conducted with a tandem configuration in mind. In some cases, this will require new approaches to catalyst and reactor design. For example, as opposed to simply maximizing selectivity toward a single product, the tandem processes must control product formation while considering the amounts of unconverted reactants. Improving the tandem processes also requires tuning key competing reactions, i.e., CO_2-ODHE vs DRE and hydroformylation vs hydrogenation in the TC-based cases, CO_2RR to C_2H_4 and CO vs HER in the EC-based cases, and C−C vs C−O recombination reactions involving C_2H_5 in the P-TC case. The downstream reactors and catalysts must also be designed for compatibility with the outlet stream of the first reactor: for example, considering the potential effects of unconverted reactants, undesired byproducts, and moisture (from CO_2-ODHE or CO_2RR) or plasma−catalyst interactions (in the P-TC scheme).

Furthermore, the CO_2-based tandem strategy for C_3 Oxys can be extended to a range of other multicarbon, value-added liquid products. The effluent from the first reactors is essentially a mixture of unconverted reactants (e.g., CO_2, C_2H_6, and/or H_2O) and products (e.g., C_2H_4, CO, H_2, and/or H_2O); thus, there remain many opportunities for incorporating other reaction chemistries in the downstream reactors. For example, carboxylic acids can be obtained via a direct or CO_2-mediated hydrocarboxylation process (i.e., $C_2H_4 + CO + H_2O \rightarrow CH_3CH_2COOH$ or $C_2H_4 + CO_2 + H_2 \rightarrow CH_3CH_2COOH$). Despite the similar thermodynamic characteristics with hydroformylation, successful demonstrations of heterogeneous hydrocarboxylation have been rarely reported. Future efforts should focus on mechanistic studies for the kinetically relevant step(s) and, in turn, develop proof-of-concept catalysts. Aromatics can also be obtained via a downstream aromatization reaction of ethylene (i.e., $3\ C_2H_4 \rightarrow C_6H_6 + 3\ H_2$) by virtue of the synergistic Brønsted acid−Lewis acid functions of zeolite-based catalysts. Such types of catalysts should be advanced with regard to coking resistance and hydrothermal stability for the tandem processes. Electrochemical CO reduction to acetate, ethanol, and other C_{2+} oxygenates also remains a promising approach to tandem EC-EC CO_2 electrolysis; however, the desired liquid products must be generated with much higher concentrations and purities to reduce the energy consumption of product separation. Equally important to the two-step tandem strategies, it is worthwhile to investigate the coupling of thermo/electro/plasma/bio/photochemical processes within a single reactor to bridge the so-called "thermodynamic gap" and achieve a one-pot conversion process. We hope that this Perspective will stimulate future research efforts exploring the vast possibilities of tandem CO_2 conversion strategies.

■ ASSOCIATED CONTENT

Supporting Information

The Supporting Information is available free of charge at https://pubs.acs.org/doi/10.1021/jacsau.2c00533.

Calculations of C_3 oxygenate yields, practical and theoretical energy costs, and net CO_2 emissions (PDF)

■ AUTHOR INFORMATION

Corresponding Author

Jingguang G. Chen − *Department of Chemical Engineering, Columbia University, New York, New York 10027, United States; Chemistry Division, Brookhaven National Laboratory, Upton, New York 11973, United States;* orcid.org/0000-0002-9592-2635; Email: jgchen@columbia.edu

Authors

Akash N. Biswas − *Department of Chemical Engineering, Columbia University, New York, New York 10027, United States;* orcid.org/0000-0003-0105-8805

Lea R. Winter − *Department of Chemical and Environmental Engineering, Yale University, New Haven, Connecticut 06520, United States;* orcid.org/0000-0002-6409-788X

Zhenhua Xie − *Department of Chemical Engineering, Columbia University, New York, New York 10027, United States; Chemistry Division, Brookhaven National Laboratory, Upton, New York 11973, United States*

Complete contact information is available at: https://pubs.acs.org/10.1021/jacsau.2c00533

Author Contributions

A.N.B., L.R.W., and Z.X. contributed equally.

Notes

The authors declare no competing financial interest.

■ ACKNOWLEDGMENTS

This research was supported by the U.S. Department of Energy, Office of Basic Energy Sciences, Catalysis Science Program (Grant No. DE-FG02-13ER16381 and Contract No. DE-SC0012704).

■ REFERENCES

(1) Intergovernmental Panel on Climate Change. *Special Report: Global Warming of 1.5°C*; Intergovernmental Panel on Climate Change, 2018. https://www.ipcc.ch/sr15/ (accessed 2022-09-01).

(2) *Industrial Alcohol Market Information*. Market Research Future. https://www.marketresearchfuture.com/reports/industrial-alcohol-market-5787 (accessed 2022-09-01).

(3) *Global Aldehyde Market*. Market Research Future. https://www.marketresearchfuture.com/reports/aldehyde-market-2356 (accessed 2022-09−01).

(4) Qian, Y.; Guo, J.; Zhang, Y.; Tao, W.; Lu, X. Combustion and Emission Behavior of N-Propanol as Partially Alternative Fuel in a Direct Injection Spark Ignition Engine. *Appl. Therm. Eng.* **2018**, *144*, 126−136.

(5) Jouny, M.; Luc, W.; Jiao, F. General Techno-Economic Analysis of CO_2 Electrolysis Systems. *Ind. Eng. Chem. Res.* **2018**, *57* (6), 2165−2177.

(6) Franke, R.; Selent, D.; Börner, A. Applied Hydroformylation. *Chem. Rev.* **2012**, *112* (11), 5675−5732.

(7) *Hydrogen Fuel Basics*. U.S. Department of Energy. https://www.energy.gov/eere/fuelcells/hydrogen-fuel-basics (accessed 2022-09-01).

(8) Tackett, B. M.; Gomez, E.; Chen, J. G. Net Reduction of CO_2 via Its Thermocatalytic and Electrocatalytic Transformation Reactions in Standard and Hybrid Processes. *Nat. Catal.* **2019**, *2* (5), 381−386.

(9) Xie, Z.; Xu, Y.; Xie, M.; Chen, X.; Lee, J. H.; Stavitski, E.; Kattel, S.; Chen, J. G. Reactions of CO_2 and Ethane Enable CO Bond Insertion for Production of C3 Oxygenates. *Nat. Commun.* **2020**, *11*, 1887−1887.

(10) Xie, Z.; Guo, H.; Huang, E.; Mao, Z.; Chen, X.; Liu, P.; Chen, J. G. Catalytic Tandem CO_2-Ethane Reactions and Hydroformylation for C3 Oxygenate Production. *ACS Catal.* **2022**, *12* (14), 8279−8290.

(11) Biswas, A. N.; Winter, L. R.; Loenders, B.; Xie, Z.; Bogaerts, A.; Chen, J. G. Oxygenate Production from Plasma-Activated Reaction of CO_2 and Ethane. *ACS Energy Lett.* **2022**, *7* (1), 236−241.

(12) Biswas, A. N.; Xie, Z.; Xia, R.; Overa, S.; Jiao, F.; Chen, J. G. Tandem Electrocatalytic-Thermocatalytic Reaction Scheme for CO_2 Conversion to C_3 Oxygenates. *ACS Energy Lett.* **2022**, *7* (9), 2904−2910.

(13) Romero Cuellar, N. S.; Scherer, C.; Kaçkar, B.; Eisenreich, W.; Huber, C.; Wiesner-Fleischer, K.; Fleischer, M.; Hinrichsen, O. Two-Step Electrochemical Reduction of CO_2 towards Multi-Carbon Products at High Current Densities. *J. CO2 Util.* **2020**, *36*, 263−275.

(14) Bullin, K.; Krouskop, P.*Composition Variety Complicates Processing Plans for US Shale Gas*. https://www.bre.com/PDF/Composition-Variety-Complicates-Processing-Plans-for-US-Shale-Gas.pdf.

(15) Biswas, A. N.; Xie, Z.; Chen, J. G. Can CO_2-Assisted Alkane Dehydrogenation Lead to Negative CO_2 Emissions? *Joule* **2022**, *6* (2), 269−273.

(16) Wang, S.; Zhu, Z. H. Catalytic Conversion of Alkanes to Olefins by Carbon Dioxide Oxidative Dehydrogenation - A Review. *Energy Fuels* **2004**, *18* (4), 1126−1139.

(17) Li, G.; Liu, C.; Cui, X.; Yang, Y.; Shi, F. Oxidative Dehydrogenation of Light Alkanes with Carbon Dioxide. *Green Chem.* **2021**, *23* (2), 689−707.

(18) Myint, M.; Yan, B.; Wan, J.; Zhao, S.; Chen, J. G. Reforming and Oxidative Dehydrogenation of Ethane with CO_2 as a Soft Oxidant over Bimetallic Catalysts. *J. Catal.* **2016**, *343*, 168−177.

(19) Gärtner, C. A.; van Veen, A. C.; Lercher, J. A. Oxidative Dehydrogenation of Ethane: Common Principles and Mechanistic Aspects. *ChemCatChem.* **2013**, *5* (11), 3196−3217.

(20) Hood, D. M.; Johnson, R. A.; Carpenter, A. E.; Younker, J. M.; Vinyard, D. J.; Stanley, G. G. Highly Active Cationic Cobalt(II) Hydroformylation Catalysts. *Science* **2020**, *367* (6477), 542−548.

(21) Cole-Hamilton, D. J. Homogeneous Catalysis-New Approaches to Catalyst Separation, Recovery, and Recycling. *Science* **2003**, *299* (5613), 1702−1706.

(22) Mao, Z.; Xie, Z.; Chen, J. G. Comparison of Heterogeneous Hydroformylation of Ethylene and Propylene over $RhCo_3$/MCM-41 Catalysts. *ACS Catal.* **2021**, *11* (23), 14575−14585.

(23) Ro, I.; Xu, M.; Graham, G. W.; Pan, X.; Christopher, P. Synthesis of Heteroatom Rh-ReO_x Atomically Dispersed Species on Al_2O_3 and Their Tunable Catalytic Reactivity in Ethylene Hydroformylation. *ACS Catal.* **2019**, *9* (12), 10899−10912.

(24) Ro, I.; Qi, J.; Lee, S.; Xu, M.; Yan, X.; Xie, Z.; Zakem, G.; Morales, A.; Chen, J. G.; Pan, X.; Vlachos, D. G.; Caratzoulas, S.; Christopher, P. Bifunctional Hydroformylation on Heterogeneous Rh-WOx Pair Site Catalysts. *Nature* **2022**, *609* (7926), 287−292.

(25) Liu, B.; Wang, Y.; Huang, N.; Lan, X.; Xie, Z.; Chen, J. G.; Wang, T. Heterogeneous Hydroformylation of Alkenes by Rh-Based Catalysts. *Chem.* **2022**, *8* (10), 2630−2658.

(26) Benson, S. W. III - Bond Energies. *J. Chem. Educ.* **1965**, *42* (9), 502−518.

(27) Bogaerts, A.; Neyts, E. C. Plasma Technology: An Emerging Technology for Energy Storage. *ACS Energy Lett.* **2018**, *3* (4), 1013−1027.

(28) Wang, Y.; Yang, W.; Xu, S.; Zhao, S.; Chen, G.; Weidenkaff, A.; Hardacre, C.; Fan, X.; Huang, J.; Tu, X. Shielding Protection by Mesoporous Catalysts for Improving Plasma-Catalytic Ambient Ammonia Synthesis. *J. Am. Chem. Soc.* **2022**, *144* (27), 12020−12031.

(29) Gómez-Ramírez, A.; Rico, V. J.; Cotrino, J.; González-Elipe, A. R.; Lambert, R. M. Low Temperature Production of Formaldehyde from Carbon Dioxide and Ethane by Plasma-Assisted Catalysis in a Ferroelectrically Moderated Dielectric Barrier Discharge Reactor. *ACS Catal.* **2014**, *4* (2), 402−408.

(30) Peng, C.; Luo, G.; Zhang, J.; Chen, M.; Wang, Z.; Sham, T. K.; Zhang, L.; Li, Y.; Zheng, G. Double Sulfur Vacancies by Lithium Tuning Enhance CO_2 Electroreduction to n-Propanol. *Nat. Commun.* **2021**, *12*, 1580.

(31) Lv, J. J.; Jouny, M.; Luc, W.; Zhu, W.; Zhu, J. J.; Jiao, F. A Highly Porous Copper Electrocatalyst for Carbon Dioxide Reduction. *Adv. Mater.* **2018**, *30* (49), 1803111.

(32) Zhang, B.; Zhang, J.; Hua, M.; Wan, Q.; Su, Z.; Tan, X.; Liu, L.; Zhang, F.; Chen, G.; Tan, D.; Cheng, X.; Han, B.; Zheng, L.; Mo, G. Highly Electrocatalytic Ethylene Production from CO_2 on Nano-defective Cu Nanosheets. *J. Am. Chem. Soc.* **2020**, *142* (31), 13606−13613.

(33) Li, F.; Thevenon, A.; Rosas-Hernández, A.; Wang, Z.; Li, Y.; Gabardo, C. M.; Ozden, A.; Dinh, C. T.; Li, J.; Wang, Y.; Edwards, J. P.; Xu, Y.; McCallum, C.; Tao, L.; Liang, Z.-Q.; Luo, M.; Wang, X.; Li, H.; O'Brien, C. P.; Tan, C.-S.; Nam, D.-H.; Quintero-Bermudez, R.; Zhuang, T.-T.; Li, Y. C.; Han, Z.; Britt, R. D.; Sinton, D.; Agapie, T.; Peters, J. C.; Sargent, E. H. Molecular Tuning of CO_2-to-Ethylene Conversion. *Nature* **2020**, *577*, 509−513.

(34) Dinh, C.-T.; Burdyny, T.; Kibria, M. G.; Seifitokaldani, A.; Gabardo, C. M.; García de Arquer, F. P.; Kiani, A.; Edwards, J. P.; De Luna, P.; Bushuyev, O. S.; Zou, C.; Quintero-Bermudez, R.; Pang, Y.; Sinton, D.; Sargent, E. H. CO_2 Electroreduction to Ethylene via Hydroxide-Mediated Copper Catalysis at an Abrupt Interface. *Science* **2018**, *360* (6390), 783−787.

(35) Bagger, A.; Ju, W.; Varela, A. S.; Strasser, P.; Rossmeisl, J. Electrochemical CO_2 Reduction: A Classification Problem. *ChemPhysChem* **2017**, *18* (22), 3266−3273.

(36) Hori, Y.Electrochemical CO_2 Reduction on Metal Electrodes. In *Modern Aspects of Electrochemistry*; Springer: 2008; pp 89−189.

(37) Nitopi, S.; Bertheussen, E.; Scott, S. B.; Liu, X.; Engstfeld, A. K.; Horch, S.; Seger, B.; Stephens, I. E. L.; Chan, K.; Hahn, C.; Nørskov, J. K.; Jaramillo, T. F.; Chorkendorff, I. Progress and Perspectives of Electrochemical CO_2 Reduction on Copper in Aqueous Electrolyte. *Chem. Rev.* **2019**, *119* (12), 7610−7672.

(38) Zheng, Y.; Vasileff, A.; Zhou, X.; Jiao, Y.; Jaroniec, M.; Qiao, S.-Z. Understanding the Roadmap for Electrochemical Reduction of CO_2 to Multi-Carbon Oxygenates and Hydrocarbons on Copper-Based Catalysts. *J. Am. Chem. Soc.* **2019**, *141* (19), 7646−7659.

(39) Zhang, H.; Li, J.; Cheng, M.-J.; Lu, Q. CO Electroreduction: Current Development and Understanding of Cu-Based Catalysts. *ACS Catal.* **2019**, *9* (1), 49−65.

(40) Gao, F.-Y.; Bao, R.-C.; Gao, M.-R.; Yu, S.-H. Electrochemical CO_2-to-CO Conversion: Electrocatalysts, Electrolytes, and Electrolyzers. *J. Mater. Chem. A* **2020**, *8* (31), 15458−15478.

(41) Jouny, M.; Luc, W.; Jiao, F. High-Rate Electroreduction of Carbon Monoxide to Multi-Carbon Products. *Nat. Catal.* **2018**, *1*, 748−755.

(42) Li, J.; Wang, Z.; McCallum, C.; Xu, Y.; Li, F.; Wang, Y.; Gabardo, C. M.; Dinh, C.-T.; Zhuang, T.-T.; Wang, L.; Howe, J. Y.; Ren, Y.; Sargent, E. H.; Sinton, D. Constraining CO Coverage on

https://doi.org/10.1021/jacsau.2c00533
JACS Au 2023, 3, 293−305

Copper Promotes High-Efficiency Ethylene Electroproduction. *Nat. Catal.* **2019**, *2*, 1124−1131.
(43) Ripatti, D. S.; Veltman, T. R.; Kanan, M. W. Carbon Monoxide Gas Diffusion Electrolysis That Produces Concentrated C_2 Products with High Single-Pass Conversion. *Joule* **2019**, *3* (1), 240−256.
(44) Jouny, M.; Hutchings, G. S.; Jiao, F. Carbon Monoxide Electroreduction as an Emerging Platform for Carbon Utilization. *Nat. Catal.* **2019**, *2*, 1062−1070.
(45) Xia, R.; Lv, J.-J.; Ma, X.; Jiao, F. Enhanced Multi-Carbon Selectivity via CO Electroreduction Approach. *J. Catal.* **2021**, *398*, 185−191.
(46) Romero Cuellar, N. S.; Wiesner-Fleischer, K.; Fleischer, M.; Rucki, A.; Hinrichsen, O. Advantages of CO over CO_2 as Reactant for Electrochemical Reduction to Ethylene, Ethanol and n-Propanol on Gas Diffusion Electrodes at High Current Densities. *Electrochim. Acta* **2019**, *307*, 164−175.
(47) Ozden, A.; Wang, Y.; Li, F.; Luo, M.; Sisler, J.; Thevenon, A.; Rosas-Hernández, A.; Burdyny, T.; Lum, Y.; Yadegari, H.; Agapie, T.; Peters, J. C.; Sargent, E. H.; Sinton, D. Cascade CO_2 Electroreduction Enables Efficient Carbonate-Free Production of Ethylene. *Joule* **2021**, *5* (3), 706−719.
(48) Theaker, N.; Strain, J. M.; Kumar, B.; Brian, J. P.; Kumari, S.; Spurgeon, J. M. Heterogeneously Catalyzed Two-Step Cascade Electrochemical Reduction of CO_2 to Ethanol. *Electrochim. Acta* **2018**, *274*, 1−8.
(49) Overa, S.; Feric, T. G.; Park, A.-H.; Jiao, F. Tandem and Hybrid Processes for Carbon Dioxide Utilization. *Joule* **2021**, *5* (1), 8−13.
(50) Hann, E. C.; Overa, S.; Harland-Dunaway, M.; Narvaez, A. F.; Le, D. N.; Orozco-Cárdenas, M. L.; Jiao, F.; Jinkerson, R. E. A Hybrid Inorganic-Biological Artificial Photosynthesis System for Energy-Efficient Food Production. *Nat. Food* **2022**, *3* (6), 461−471.
(51) Morales-Guio, C. G.; Cave, E. R.; Nitopi, S. A.; Feaster, J. T.; Wang, L.; Kuhl, K. P.; Jackson, A.; Johnson, N. C.; Abram, D. N.; Hatsukade, T.; Hahn, C.; Jaramillo, T. F. Improved CO_2 Reduction Activity towards C_{2+} Alcohols on a Tandem Gold on Copper Electrocatalyst. *Nat. Catal.* **2018**, *1* (10), 764−771.
(52) Chen, C.; Li, Y.; Yu, S.; Louisia, S.; Jin, J.; Li, M.; Ross, M. B.; Yang, P. Cu-Ag Tandem Catalysts for High-Rate CO_2 Electrolysis toward Multicarbons. *Joule* **2020**, *4* (8), 1688−1699.
(53) She, X.; Zhang, T.; Li, Z.; Li, H.; Xu, H.; Wu, J. Tandem Electrodes for Carbon Dioxide Reduction into C_{2+} Products at Simultaneously High Production Efficiency and Rate. *Cell Rep. Phys. Sci.* **2020**, *1* (4), 100051.
(54) Li, J.; Che, F.; Pang, Y.; Zou, C.; Howe, J. Y.; Burdyny, T.; Edwards, J. P.; Wang, Y.; Li, F.; Wang, Z.; De Luna, P.; Dinh, C.-T.; Zhuang, T.-T.; Saidaminov, M. I.; Cheng, S.; Wu, T.; Finfrock, Y. Z.; Ma, L.; Hsieh, S.-H.; Liu, Y.-S.; Botton, G. A.; Pong, W.-F.; Du, X.; Guo, J.; Sham, T.-K.; Sargent, E. H.; Sinton, D. Copper Adparticle Enabled Selective Electrosynthesis of N-Propanol. *Nat. Commun.* **2018**, *9*, 4614.
(55) Zhuang, T.-T.; Pang, Y.; Liang, Z.-Q.; Wang, Z.; Li, Y.; Tan, C.-S.; Li, J.; Dinh, C. T.; De Luna, P.; Hsieh, P.-L.; Burdyny, T.; Li, H.-H.; Liu, M.; Wang, Y.; Li, F.; Proppe, A.; Johnston, A.; Nam, D.-H.; Wu, Z.-Y.; Zheng, Y.-R.; Ip, A. H.; Tan, H.; Chen, L.-J.; Yu, S.-H.; Kelley, S. O.; Sinton, D.; Sargent, E. H. Copper Nanocavities Confine Intermediates for Efficient Electrosynthesis of C3 Alcohol Fuels from Carbon Monoxide. *Nat. Catal.* **2018**, *1*, 946−951.
(56) Pang, Y.; Li, J.; Wang, Z.; Tan, C.-S.; Hsieh, P.-L.; Zhuang, T.-T.; Liang, Z.-Q.; Zou, C.; Wang, X.; De Luna, P.; Edwards, J. P.; Xu, Y.; Li, F.; Dinh, C.-T.; Zhong, M.; Lou, Y.; Wu, D.; Chen, L.-J.; Sargent, E. H.; Sinton, D. Efficient Electrocatalytic Conversion of Carbon Monoxide to Propanol Using Fragmented Copper. *Nat. Catal.* **2019**, *2*, 251−258.
(57) U.S. Energy Information Administration. *How much carbon dioxide is produced per kilowatthour of U.S. electricity generation?*https://www.eia.gov/tools/faqs/faq.php?id=74&t=11.
(58) Motte, J.; Mahmoud, M.; Nieder-Heitmann, M.; Vleeming, H.; Thybaut, J. W.; Poissonnier, J.; Alvarenga, R. A. F.; Nachtergaele, P.; Dewulf, J. Environmental Performance Assessment of a Novel Process Concept for Propanol Production from Widely Available and Wasted Methane Sources. *Ind. Eng. Chem. Res.* **2022**, *61* (30), 11071−11079.
(59) Rabinowitz, J. A.; Kanan, M. W. The Future of Low-Temperature Carbon Dioxide Electrolysis Depends on Solving One Basic Problem. *Nat. Commun.* **2020**, *11*, 5231.
(60) Ma, M.; Clark, E. L.; Therkildsen, K. T.; Dalsgaard, S.; Chorkendorff, I.; Seger, B. Insights into the Carbon Balance for CO_2 Electroreduction on Cu Using Gas Diffusion Electrode Reactor Designs. *Energy Environ. Sci.* **2020**, *13* (3), 977−985.
(61) Kutz, R. B.; Chen, Q.; Yang, H.; Sajjad, S. D.; Liu, Z.; Masel, I. R. Sustainion Imidazolium-Functionalized Polymers for Carbon Dioxide Electrolysis. *Energy Technol.* **2017**, *5* (6), 929−936.
(62) Li, Y. C.; Zhou, D.; Yan, Z.; Gonçalves, R. H.; Salvatore, D. A.; Berlinguette, C. P.; Mallouk, T. E. Electrolysis of CO_2 to Syngas in Bipolar Membrane-Based Electrochemical Cells. *ACS Energy Lett.* **2016**, *1* (6), 1149−1153.
(63) Salvatore, D. A.; Weekes, D. M.; He, J.; Dettelbach, K. E.; Li, Y. C.; Mallouk, T. E.; Berlinguette, C. P. Electrolysis of Gaseous CO_2 to CO in a Flow Cell with a Bipolar Membrane. *ACS Energy Lett.* **2018**, *3* (1), 149−154.
(64) Yan, Z.; Hitt, J. L.; Zeng, Z.; Hickner, M. A.; Mallouk, T. E. Improving the Efficiency of CO_2 Electrolysis by Using a Bipolar Membrane with a Weak-Acid Cation Exchange Layer. *Nat. Chem.* **2021**, *13*, 33−40.
(65) Song, Y.; Zhang, X.; Xie, K.; Wang, G.; Bao, X. High-Temperature CO_2 Electrolysis in Solid Oxide Electrolysis Cells: Developments, Challenges, and Prospects. *Adv. Mater.* **2019**, *31* (50), 1902033.
(66) Zhang, L.; Hu, S.; Zhu, X.; Yang, W. Electrochemical Reduction of CO_2 in Solid Oxide Electrolysis Cells. *J. Energy Chem.* **2017**, *26* (4), 593−601.
(67) Ozden, A.; García de Arquer, F. P.; Huang, J. E.; Wicks, J.; Sisler, J.; Miao, R. K.; O'Brien, C. P.; Lee, G.; Wang, X.; Ip, A. H.; Sargent, E. H.; Sinton, D. Carbon-Efficient Carbon Dioxide Electrolysers. *Nat. Sustain.* **2022**, *5* (7), 563−573.
(68) Wang, X.; Ou, P.; Ozden, A.; Hung, S.-F.; Tam, J.; Gabardo, C. M.; Howe, J. Y.; Sisler, J.; Bertens, K.; García de Arquer, F. P.; Miao, R. K.; O'Brien, C. P.; Wang, Z.; Abed, J.; Rasouli, A. S.; Sun, M.; Ip, A. H.; Sinton, D.; Sargent, E. H. Efficient Electrosynthesis of N-Propanol from Carbon Monoxide Using a Ag-Ru-Cu Catalyst. *Nat. Energy* **2022**, *7*, 170−176.
(69) Liu, S.; Winter, L. R.; Chen, J. G. Review of Plasma-Assisted Catalysis for Selective Generation of Oxygenates from CO_2 and CH_4. *ACS Catal.* **2020**, *10* (4), 2855−2871.